A Vector Grouping Algorithm for Liquid Crystal Tensor Field Visualization

Yang-Ming Zhu*, *Member, IEEE* and Paul A. Farrell

Department of Computer Science

Kent State University, Kent, Ohio 44242

Abstract

Tensor fields are at the heart of many science and engineering disciplines. Many tensor visualization methods separate the tensor into component eigenvectors and visualize those instead. Eigenvectors are normally ordered according to their eigenvalues: the eigenvectors corresponding to the smallest, median, or largest eigenvalues are in their corresponding groups. We showed that this ordering strategy is not desirable for liquid crystal systems and proposed a new approach where the vectors are grouped to minimize some local energy. The grouping process is reminiscent of the epitaxial expansion in the anchoring of liquid crystals on a surface. The new algorithm is successfully applied to the liquid crystal system to study the biaxiality structure near a defect.

Keywords: tensor, vector, visualization, liquid crystals

*Current address: Nuclear Medicine Division, Marconi Medical Systems, 595 Miner Road, Cleveland, Ohio 44143.

Email: yang-ming.zhu@marconi.com

1 Introduction

Tensor data sets are at the heart of many science and engineering areas such as fluid dynamics, but few methods have been proposed to visualize and understand the richness of these fields [1, 2]. The first method proposed to visualize a tensor field is to represent the tensor by an ellipsoid, the orientations of which are determined by the eigenvectors, and the relative lengths of whose axes are determined by the eigenvalues [3]. The generalization of this approach is to use a local icon to represent the tensor at various points in space. As an alternative, scalar components can be analyzed and displayed in 2D or 3D form which is not effective and may discard valuable information about the data. Motivated by their previous work on the topological representation of vector fields [4, 5], Hesselink and his coworkers recently proposed a topological approach [6, 7] which can capture the global structure of a tensor field.

A 3D tensor is a 3×3 matrix. A 3×3 matrix can be uniquely represented by three eigenvalues and their corresponding eigenvectors. The visualization of tensor fields thus can be reduced to the visualization of three vector fields and any vector visualization method can be applied to these separated vector fields. In current practice [6, 7], the vector fields are separated according to their eigenvalues, i.e. eigenvectors corresponding to the largest eigenvalues are in a group, those corresponding to the median eigenvalues are in another group, and those corresponding to the smallest eigenvalues are in yet another group. The separated vector fields can be further processed, as in the topological representation paradigm where topological skeletons are emphasized [6]. A point where two or three eigenvalues are equal is called degenerate. Tensor field lines or hyperstreamline trajectories are calculated in each separated vector field along those degenerate points. Those calculated topological skeletons can be rendered together or separately. This approach greatly reduces the display clutter and has proven to be useful in some areas.

In our research we found that the vector ordering strategy, i.e. separating eigenvectors according to the magnitude of the corresponding eigenvalues, is not appropriate for liquid crystal tensor field visualization. To remedy this, a vector grouping algorithm is developed in this paper based on the energy minimization principle. After the eigenvectors are properly grouped, any vector rendering

algorithms, including the topological skeletons, can be applied to the grouped vector fields.

The remainder of this paper is organized as follows: Section 2 describes the vector grouping algorithm with a brief discussion of its physics origin. Section 3 illustrates two examples to demonstrate that the conventional vector ordering scheme is not appropriate whereas the new strategy works well. Since liquid crystal problems are relatively unknown in the graphics and visualization community, a brief discussion is provided in the Appendix.

2 Vector grouping algorithm

The idea of this new vector grouping algorithm is to minimize the direction change in each vector group. For two unit vectors, if their directions differ slightly, their inner product has a large value (close to 1). Assume eigenvalues λ_1, λ_2, and λ_3 and their corresponding unit eigenvectors u, v, and w are given in space $(x_i, y_j, z_k), i, j, k = 0, 1, ..., N-1$. The algorithm intends to group vectors along a line, grows the ordering in a plane and then into bulk. It has the following steps:

1. At (x_0, y_0, z_0), pick three eigenvectors arbitrarily and label them as $U_{0,0,0}$, $V_{0,0,0}$, and $W_{0,0,0}$.

2. For $i = 1, 2, \cdots, N-1$, and for the six permutations of eigenvectors $(U_{i,0,0}, V_{i,0,0}, W_{i,0,0})$: $(u, v, w), (u, w, v), (v, u, w), (v, w, u), (w, u, v)$, or (w, v, u), compute

$$(U_{i-1,0,0}, U_{i,0,0})^2 + (V_{i-1,0,0}, V_{i,0,0})^2 + (W_{i-1,0,0}, W_{i,0,0})^2,$$

   where (a, b) is the inner product of vector a and b. Pick the permutation that has the largest value and swap the involved eigenvalues and eigenvectors accordingly. For example, if (w, u, v) gives the largest value, then swap u and w first and then swap u and v.

3. For $i = 0, 1, \cdots, N-1, j = 1, 2, \cdots, N-1$, and for the six permutations of (U, V, W) at (x_i, y_j, z_0), compute

$$\sum_{<x,y>} (U_{x,y,0}, U_{i,j,0})^2 + (V_{x,y,0}, V_{i,j,0})^2 + (W_{x,y,0}, W_{i,j,0})^2,$$

where $(x, y) = (i-1, j-1), (i, j-1), (i+1, j-1)$. Pick the permutation that has the largest value and swap the involved eigenvalues and eigenvectors accordingly. If some neighbors of (x_i, y_j, z_0) are missing, the associated terms are dropped out.

4. For $i = 0, 1, \cdots, N-1, j = 0, 1, \cdots, N-1, k = 1, 2, \cdots, N-1$, and for the six permutations of (U, V, W) at (x_i, y_j, z_k), compute

$$\sum_{<x,y,z>} (U_{x,y,z}, U_{i,j,k})^2 + (V_{x,y,z}, V_{i,j,k})^2 + (W_{x,y,z}, W_{i,j,k})^2,$$

where $(x, y, z) = (i-1, j-1, k-1), (i, j-1, k-1), (i+1, j-1, k-1), (i-1, j, k-1), (i, j, k-1), (i+1, j, k-1), (i-1, j+1, k-1), (i, j+1, k-1), (i+1, j+1, k-1)$. Pick the permutation that has the largest value and swap the involved eigenvalues and eigenvectors accordingly. If some neighbors of (x_i, y_j, z_k) are missing, the associated terms are dropped out.

In step 2 the ordering grows along a line. In step 3 the ordering grows from a line. In step 3 one may group the vectors in two edges and then grow the ordering into bulk, or group around four edges first, then shrink to the center. In step 4 the ordering grows from a plane. All the nine neighbors from the previous plane of the current point are considered. For simplicity, one may just consider five neighbors $(i, j, k-1), (i-1, j, k-1), (i+1, j, k-1), (i, j+1, k-1)$, and $(i, j-1, k-1)$. Again, there are other possibilities to group the vectors along different planes, and from different corners.

Since u and $-u$ both are eigenvectors of the corresponding eigenvalue, we compute the squared inner products while grouping. If one wants to take into account the eigenvalues while grouping, $\lambda_{U_{i-1}} \lambda_{U_i} (U_{i-1}, U_i)^2$ like can be used. We also found that if the absolute value of the inner product is used, similar results can be achieved.

Our algorithm has its physical basis. For an Ising model with two spin states (up and down), the Hamiltonian is [8]

$$H = -J \sum_{<i,j>} S_i \cdot S_j,$$

where positive J is the molecular interaction, and S_i is the spin on lattice i. If the state is a vector, then

$$H = -J \sum_{<i,j>} (v_i, v_j),$$

where v_i is the vector state on lattice i. For a liquid crystal system in particular [9],

$$H = -J \sum_{<i,j>} (v_i, v_j)^2$$

since $-\mathbf{v}$ and $\mathbf{v}$ are equivalent. Similarly, if the state is described by a tensor, we define a Hamiltonian as

$$H = -J \sum_{<i,j>} (u_i, u_j)^2 + (v_i, v_j)^2 + (w_i, w_j)^2,$$

where u_i, v_i, w_i are the eigenvectors on lattice i. To find the most favorable state, this Hamiltonian can be minimized. Minimizing this Hamiltonian is the same as the maximization criterion used in the grouping algorithm. It is worth noting that the approach used in the grouping algorithm is similar to the epitaxial growth of liquid crystals on a surface [10].

3 Examples and discussion

In this section we show two examples of the application of the vector grouping algorithm to liquid crystal tensor field visualization. Traditionally the liquid crystal is described by a vector field [11]. That implies that liquid crystals are uniaxial. However, experimental results indicate that liquid crystals may be biaxial [11, 12]. Theoretical results also show that, close to a topological defect, the liquid crystal is biaxial [13]. The vector representation is not adequate for this biaxial field, instead a tensor field is used. If none of the three eigenvalues are equal, the liquid crystal is biaxial; if two of them are equal, it is uniaxial; and if all three are equal, it is isotropic. Liquid crystals are uniaxial in most of the cases. Thus in liquid crystal tensor field visualization the uniaxial case is considered normal. If defects are involved, then some biaxial or isotropic regions are embedded in the uniaxial background. The changes of eigenvalues in space are of interest.

A 2D data set was generated by a SIMD machine implementing the solver of the Landau-de Gennes model (see the Appendix for detail). The temperature was 0.65 and the data set size was

65×65. Two defects of strength $\frac{1}{2}$ were introduced in the calculation.

Figure 1 shows the rendering result when eigenvectors are separated based on the relative strength of their eigenvalues: eigenvectors corresponding to the largest, medium, and smallest eigenvalues are rendered to the right, middle and left viewports, respectively. In the following examples, the viewports and eigenvalues have the same relation when the eigenvectors are ordered based on their eigenvalues. To reduce display clutter the vectors on every other grid in both dimensions are displayed.

In the right viewport, the defects (singular points) introduced in the calculation are obvious and labeled with crosses. Those defects are also visible in the left viewport (but not labeled). The other four crosses labeled in the left viewport are artifacts due to the grouping scheme used. Those disordered vectors are also visible in the middle viewport at the corresponding positions close to the four corners. The distortion is more pronounced in orthogonal projection with the stride of 1. These distortions are not favorable energetically. In fact, at these corners the biaxiality is weak and we would not expect such a big distortion. Fig 2 shows the rendering results using our grouping algorithm. The situation in four corners is evidently improved. Our new grouping strategy eliminates the false defects.

The eigenvalues are color coded in Figs. 1 and 2. From the right and left viewports, one can clearly observe that the eigenvalues are decreasing close to the defects. Since eigenvalues reflect the ordering of the field, the ordering decreases approaching the defects.

A 3D data set was generated by a cluster of workstations which implements the solver for the 3D case. The size of this data set was $21 \times 21 \times 21$. The temperature was 0.328. Currently we are unable to generate bigger data set such as $100 \times 100 \times 100$. A defect with the strength of 1 was introduced at the center of the field during the computation. Homeotropic surface anchoring conditions were assumed. That is, all major eigenvectors are perpendicular to the surface, and more or less, they are in the radial direction in the bulk.

Figure 3 shows the vector fields at the 12th slice parallel to the XOY plane. The eigenvectors are separated according to the magnitude of their eigenvalues. Since the defect is at the center of the

field (in the 10th slice), we do not expect to see any defects, which is confirmed by the major vector component in the right viewport. The major eigenvectors are perpendicular to the paper surface in the center and tilt gradually until parallel to the paper surface towards the confining boundary. The ordering decreases close to the defect. The rendering in the left and middle viewports is physically unacceptable. Along the surface, these vector fields should have a more or less regular configuration by simple symmetry argument. In the bulk, the change of vector direction should be smooth. In the left and middle viewports of Fig. 3, however, the discontinuity of the vector fields along the edge and in the bulk is evident.

Figure 4 shows the rendering of the same slice. The vectors fields were grouped by using the vector grouping algorithm. The vectors in the central plane (10th plane) were grouped first and then grown in two opposite directions in Z. In all these calculations, eigenvalues were also taken into account, as we discussed earlier. There is no difference detected in the right viewport, but the rendering of the left and middle viewports is apparently different. Unlike the vectors in Fig. 4, the vectors along the edges are in a regular pattern in both the left and middle viewports. The regularity of the vector field in the middle viewport is greatly improved compared to that in Fig. 4. The regularity of the vectors in the left viewport is also arguably improved. Some irregularity in the left viewport is due to the effect of projection: if the vectors in the irregular region are replaced by those in the middle viewport at the corresponding positions, the irregularity still exists. The data set used here is relatively small and the direction changes of a vector in each group is larger. This effect of projection is inevitable. However, there are vectors misgrouped, e.g. the vector immediately above the vector at the center. This misgrouping is hard to avoid due to the limited amount of data points and rapid change of direction between neighboring data points. Moreover, as the distance to the initial plane becomes large, the separated eigenvectors become random. Nevertheless, our grouping scheme reduces the amount of irregularity in the grouped vector fields and gives a reasonable result.

The grouping result of our algorithm may depend on the direction in which the ordering grows. In fact our algorithm is a special implementation of the energy minimization principle. In that

implementation the neighbors whose vectors have not been grouped are not considered. An ideal implementation is to consider all neighbors where the Monte Carlo method can be exploited which is much slower than the scheme presented. If the grouping direction dependency is a problem, one can resort to the Monte Carlo method. The orientation of liquid crystals is imposed by the surface contacting them. Therefore growth from a particular direction seems reasonable.

4 Conclusion

A 3×3 tensor can be uniquely expressed by three eigenvalues and their corresponding eigenvectors. The visualization of the tensor field is equivalent to the visualization of three eigenvector fields, without loss of any information. We have shown that it is not appropriate to separate the eigenvectors of liquid crystal tensor fields based on the relative strength of their eigenvalues and then render these eigenvector fields. A vector grouping strategy was proposed to minimize the directional changes in each vector group. This strategy was successfully applied to grouping eigenvectors of 2D and 3D tensor fields. The grouped eigenvectors make sense from a physics standpoint, and any vector visualization techniques, including local icon depiction and streamline representation, can be subsequently used to render the grouped eigenvector fields.

Acknowledgements: We thank the reviewers for their constructive comments and suggestions. Thanks are also due to Dr. Arden Ruttan for providing us the 3D data set. This work was supported by the National Science Foundation under grant "A steering and visualization environment" (#9720221), by the NSF Advanced Liquid Crystalline Optical Material (ALCOM) Science and Technology Center, and by an Ohio Board of Regents Research Challenge grant.

Appendix: Liquid crystal tensor fields

Liquid crystals have different phases [11]. The nematic phase is studied most and is the focus of this paper.

The orientation of liquid crystals can be abstracted by a director field **n**, a unit vector defined

in space. The thermal average of $\mathbf{n}$ gives the director. If the director field is not a smooth function of spatial coordinates, the singular points and lines are called defects. For liquid crystals, $\mathbf{n}$ and $-\mathbf{n}$ are equivalent.

The ordering of liquid crystals is described by the ordering matrix $Q^{\alpha\beta} = \frac{1}{2} < 3n_\alpha n_\beta - \delta_{\alpha\beta} >$, where $\alpha, \beta = x, y, z$ are indices referring to the laboratory frame, and δ is a Kronecker symbol defined as $\delta = 1$ if $\alpha = \beta$ and zero otherwise. In an explicit matrix form, $Q = \frac{1}{2} < 3\mathbf{n}\mathbf{n}^T - I >$, where T is transpose and I is a unit matrix. The tensor Q is traceless and symmetric. If all its eigenvalues are equal, it is an isotropic liquid. If two of them are equal, it is a uniaxial nematic. If none of them are equal, it is biaxial.

The bulk free energy density of a liquid crystal system according to the Landau-de Gennes theory is

$$\begin{aligned} f_{bulk} = & \frac{1}{2}L_1 Q_{\alpha\beta,\gamma} Q_{\alpha\beta,\gamma} + \frac{1}{2}L_2 Q_{\alpha\beta,\beta} Q_{\alpha\gamma,\gamma} + \frac{1}{2}L_3 Q_{\alpha\beta,\beta} Q_{\alpha\gamma,\beta} + \\ & \frac{1}{2}A tr(Q^2) - \frac{1}{3}B tr(Q^3) + \frac{1}{4}C tr(Q^2)^2 + \frac{1}{5}D tr(Q^2) tr(Q^3) + \\ & \frac{1}{6}M tr(Q^3)^2 + \frac{1}{6}M' tr(Q^2)^3 - \Delta\chi H_\alpha Q_{\alpha\beta} H_\beta - \Delta\epsilon E_\alpha Q_{\alpha\beta} E_\beta \end{aligned}$$

where traditional physics conventions are used, i.e. summation over repeated indices is implied and indices separated by commas indicate partial derivatives with respective to the index after the comma. Here $L_1, L_2, L_3, A, B, C, D, M, M', H, E, \Delta\epsilon, \Delta\chi$ are physical constants.

To find the stable configuration of a liquid crystal system, one needs to minimize the Landau-de Gennes energy numerically. The computation of this system is challenging. It is desirable to implement the solver on a parallel machine or on a distributed network of workstations. The solver has already been implemented on a 16,384 processors, 512 Mbyte memory Wavetracer DTC SIMD machine for a 2D slab geometry, and on a distributed network of workstations using MPI (Message Passing Interface) in the Department of Computer Science at Kent State University.

References

[1] G.M. Nielson, H. Hagen, and H. Muller, *Scientific Visualization: Overviews, Methodologies, and Techniques*, ed. Los Alamitos, CA: IEEE Computer Society Press, 1997. Chapters 13, 16, 21.

[2] M.A. Livingston, "Visualization of rotation fields", *Proc. IEEE Visualization'97*, pp.491-494, 1997.

[3] L. Hesselink and T. Delmarcelle, *Scientific Visualization: Advances and Challenges*, chap. 26, pp.419-433, IEEE Computer Society Press, 1994.

[4] J. Helman and L. Hesselink, "Representation and display of vector field topology in fluid flow data sets", *Computer*, pp.27-36, August 1989.

[5] J. Helman and L. Hesselink, "Visualization of vector field topology in fluid flows", *IEEE Computer Graphics and Applications*, vol. 11, no. 3, pp.36-46, 1991.

[6] L. Hesselink, Y. Levy, and Y. Lavin, "The topology of symmetric, second-order 3D tensor fields", *IEEE Trans. Visualization and Computer Graphics*, vol. 3, no. 1, pp.1-11, 1997.

[7] Y. Lavin, Y. Levy, and L. Hesselink, "Singularities in nonuniform tensor fields", *Proc. IEEE Visualization'97*, pp.59-66, 1997.

[8] H.E. Stanley, *Introduction to Phase Transitions and Critical Phenomena*, Oxford: Clarendon Press, 1971.

[9] P.A. Lebwohl and G. Lasher, "Nematic liquid crystal order – A Monte Carlo calculation", *Phys. Rev. A*, vol.6, no.1, pp.426-429, 1972.

[10] J.Y Fang, Z.H. Lu, G.W. Min, Z.M. Ai, Y. Wei, and P. Stroeve, "Anchoring structure of liquid crystal monolayers on polyimide Langmuir-Blodgett films observed by scanning tunneling microscopy", *Phys. Rev. A*, vol.46, no.8, pp.4963-4965, 1992.

[11] P.G. de Gennes and J. Prost, *The Physics of Liquid Crystals*, 2nd ed., Oxford Univ. Press, 1993.

[12] S. Chandrasekhar, G.G. Nair, D.S.S. Rao, S.K. Prasad, K. Praefcke, and D. Blunk, "Schlieren textures in free standing nematic films: evidence of biaxiality", *Liq. Cryst.* vol.24, pp. 67-70, 1998.

[13] N. Schopohl and T.J. Sluckin, Defect core structure in nematic liquid crystals, *Phys. Rev. Lett.* 59, 2582 (1987).

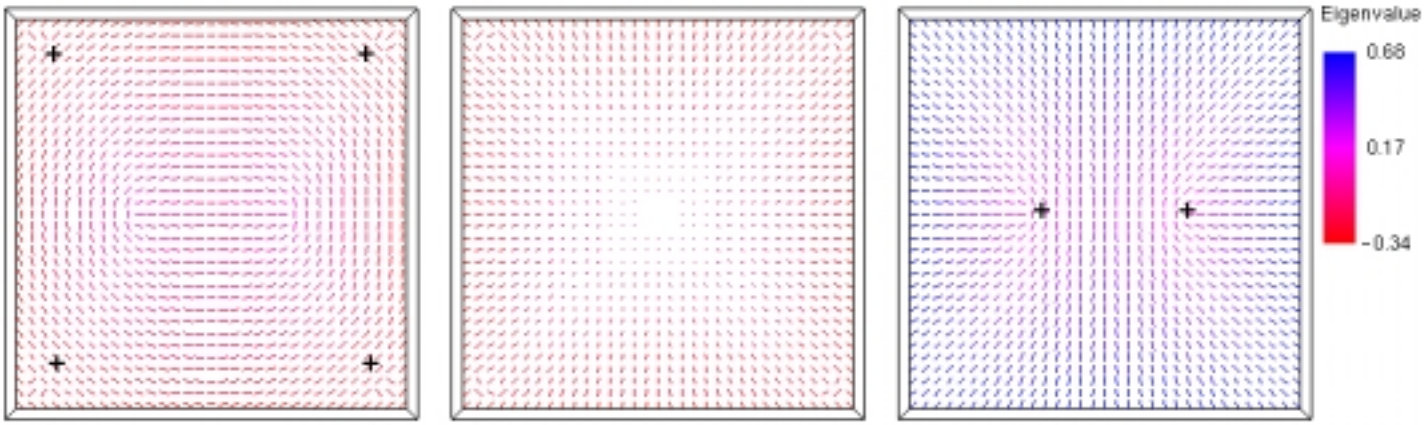

Figure 1: A 2D tensor field with two defects rendered according to the relative strength of eigenvalues. The stride is 2.

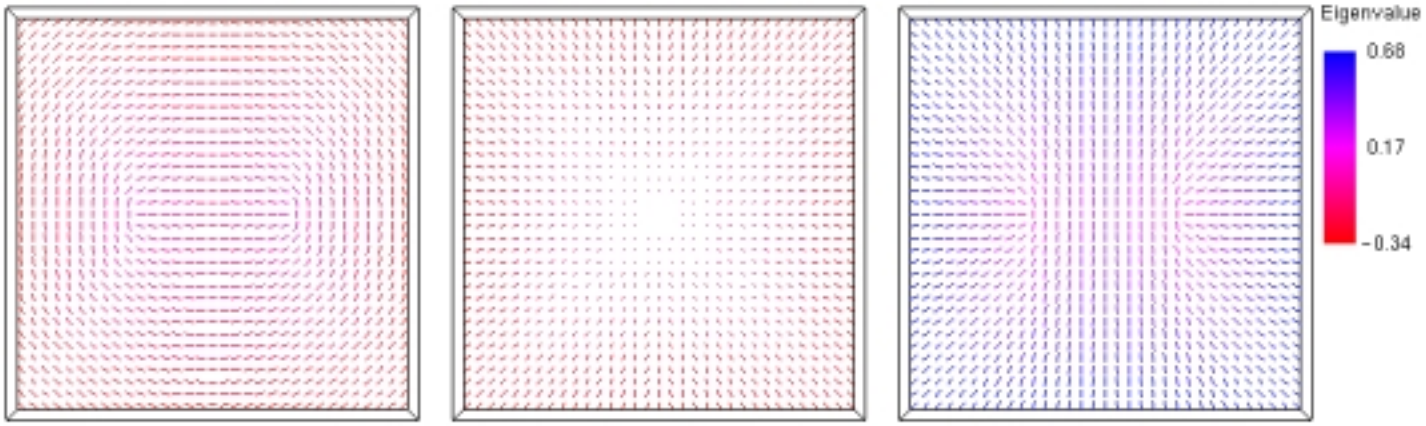

Figure 2: The same 2D tensor field as in Fig. 1 rendered using the vector grouping algorithm. The stride is 2.

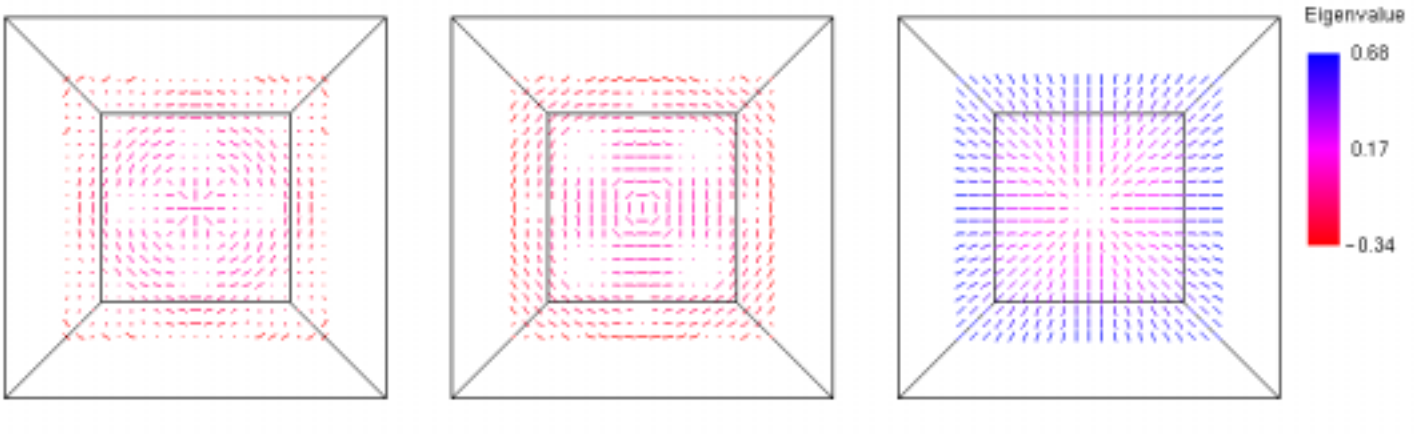

Figure 3: A 3D tensor field rendered according to the magnitude of the eigenvalues. The 12th slice parallel to the XOY plane is displayed.

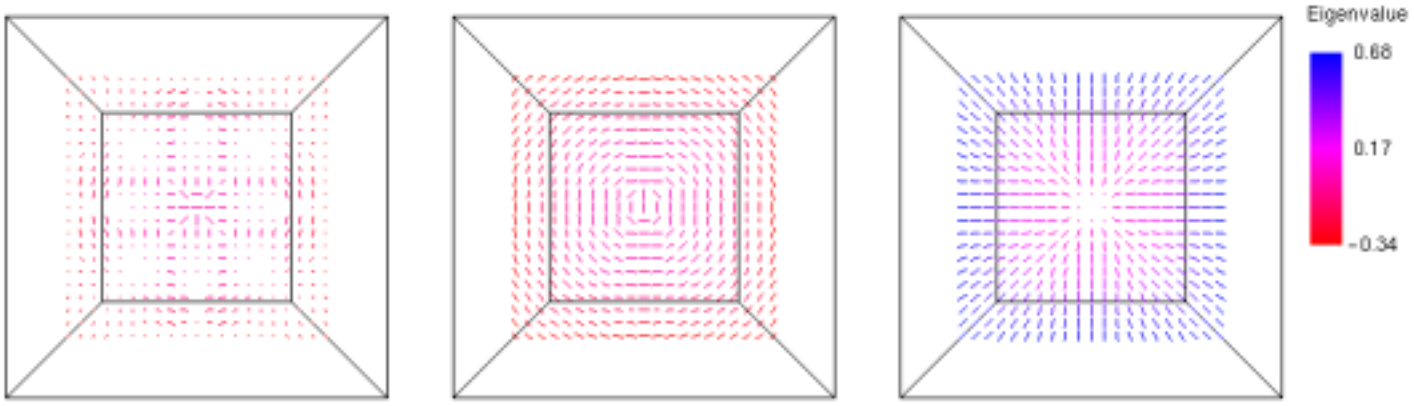

Figure 4: The same 3D tensor field as in Fig. 3 rendered with the vector grouping algorithm.